Measurement of Fission Cross Section and Angular Distributions of Fission Fragments from Neutron-Induced Fission of ^{243}Am in the Energy Range 0.3–500 MeV

A.M. Gagarski, A.S. Vorobyev,
O.A. Shcherbakov, L.A. Vaishnene

Petersburg Nuclear Physics Institute
of NRC "Kurchatov Institute", Gatchina, Russia

A.L. Barabanov

NRC "Kurchatov Institute", Moscow, Russia

T.E. Kuz'mina

Khlopin Radium Institute, St.-Petersburg, Russia

PNPI, Gatchina

NATIONAL RESEARCH CENTER "KURCHATOV INSTITUTE"

SINN-29, Dubna, Russia, May 29 – June 2, 2023

Motivation for measurements of the fission cross section of ^{243}Am

- One of the main problems in the reprocessing of spent nuclear fuel produced in modern nuclear reactors are Am and Cm isotopes due to their high activity and long half-life. Am is the most dangerous due to its high yield and high activity. ^{243}Am contributes also to the formation of ^{239}Pu. The share of ^{243}Am among other minor Am actinides is ~15% in spent fuel from thermal reactors. Today, the transmutation of nuclear waste in fast neutron reactors seems to be one of the promising ways to reduce the radiotoxicity of spent nuclear fuel
- The practical implementation of plans for both the creation of a **closed fuel cycle** based on fast nuclear reactors and the **disposal of radioactive waste** is impossible without reliable and accurate nuclear data. For example, the required accuracy of the fission cross section of ^{243}Am(n,f) is 2% when designing the sodium-cooled fast reactor (SFR) and 7% for designing the accelerator-driven minor actinide burner reactor (ADMAB) [WPEC-26, NEA No. 6410. OECD-NEA, 2008]
- The data available on the fission cross section of ^{243}Am are mainly limited to the neutron energies below 20 MeV. Most of this data was obtained using monoenergetic neutrons obtained in various reactions at accelerators. The available experimental data reveals a significant scatter, which reaches 30% in the neutron energy range of 2-5 MeV. There are practically no experimental data for neutron energies above 20 MeV. **Therefore, new measurements of the fission cross section of ^{243}Am should be made in a wide neutron energy range on neutron beams with a continuous spectrum using the time-of-flight method**

Motivation for studying the angular distributions of fission fragments

The angular distributions of fission fragments appear due to the action of two factors: 1– the ensemble of spins of fissioning nuclei must be aligned; 2– the distribution of transition states over the K-projection of the nuclear spin onto the fission axis must be non-uniform. The first factor is determined by the processes preceding fission, while the second is set by the fission mechanism itself.

- Information on fission barriers and transition state spectra on barriers. (states of highly deformed fissioning nucleus at the fission saddle point)
- Verification and developing of models for adequate description of processes in nuclei at high excitations (relative contribution of equilibrium and non-equilibrium processes into the dynamics of highly excited nuclei)
- The angular distributions data are important for precise measurements of the fission cross-sections, because it should be taken into account as efficiency correction for non 4π detectors
- Such an information for highly excited nuclei is important for development of new technologies, such as Accelerator-Driven Systems for nuclear power, nuclear waste transmutation, and etc.
- Existing data about fission fragment anisotropy have sometimes big discrepancies even for incoming neutron energies below 20 MeV, they are very scarce above 20 MeV and are practically absent for neutron energy range above 100 MeV.
  Namely, for ^{243}Am there are no such data.

Neutron TOF-spectrometer GNEIS

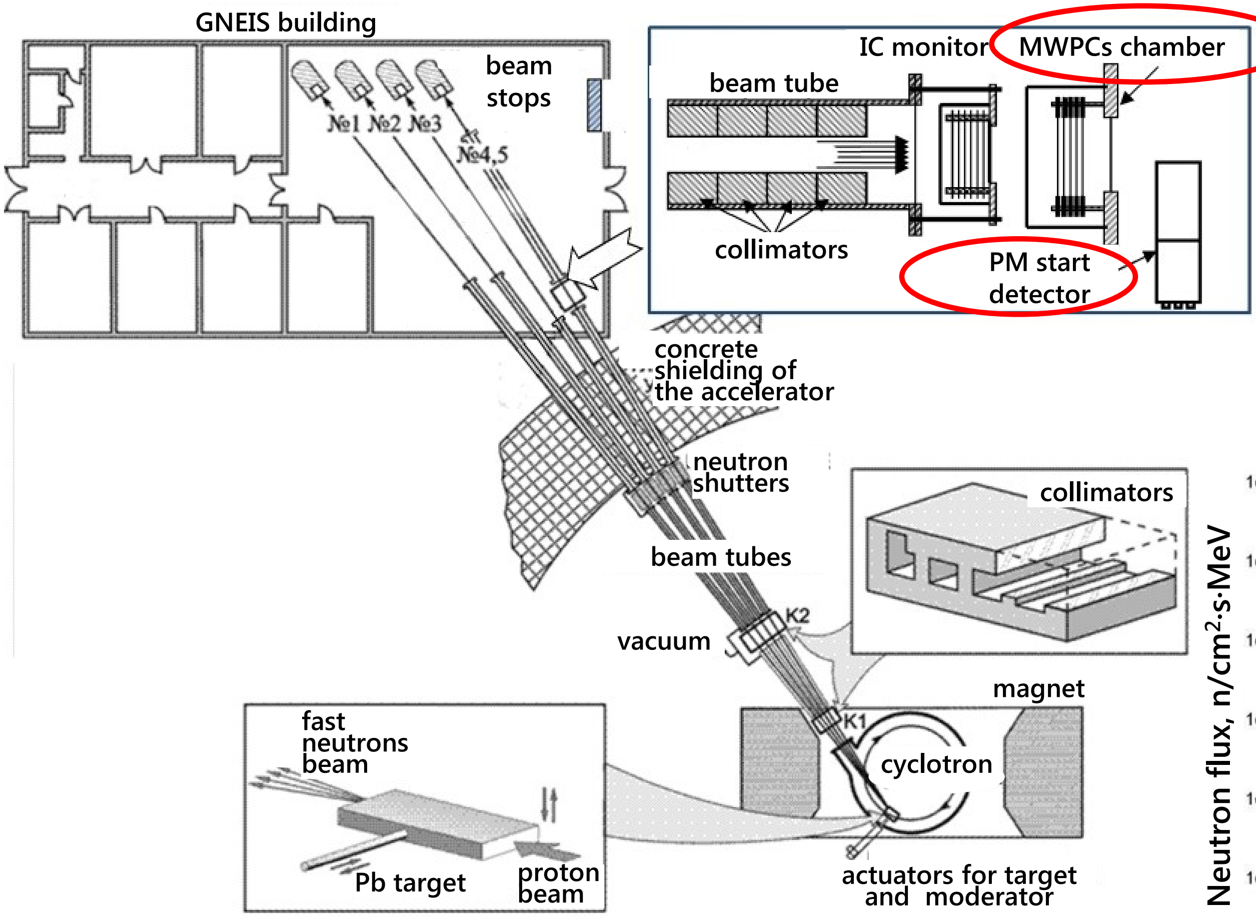

Neutron spectrum of GNEIS: from thermal to 1 GeV

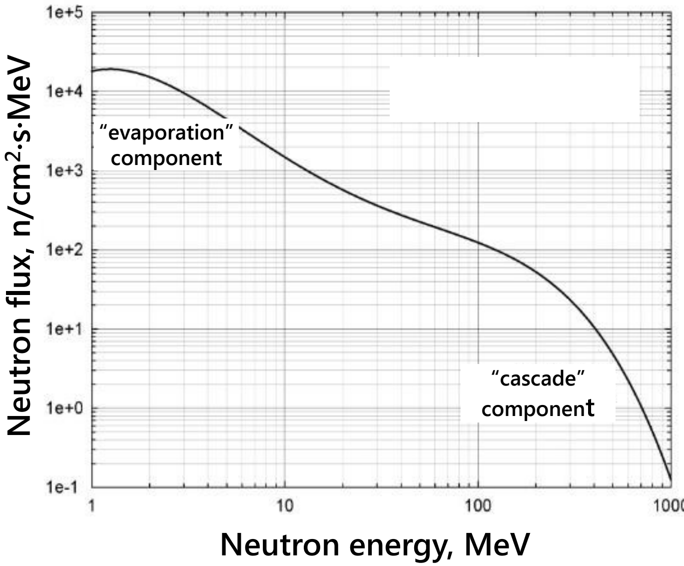

Main parameters:

$E_{protons} = 1$ GeV; Lead target; $\Delta t \approx 10$ ns;

$f \approx 50$ Hz; $\Phi \sim 3 \times 10^{14} \frac{\text{n}}{\text{s}}$; $L = 36.5$ m

$$\frac{\Delta E}{E}(1\ MeV) \approx 1\% \ ; \ \frac{\Delta E}{E}(200\ MeV) \approx 12\%$$

Experimental setup

Most often, the fission cross section of the nucleus under study is measured relative to the cross section of a reaction that is known with a high accuracy (standard cross section) such as n–p scattering, ..., and the neutron induced fission of ^{235}U.

To do this, it is necessary to place the main target and the reference target of ^{235}U

- with an exactly known ratio of number of nuclei (N_{Am3}/N_{U5})
- in the same neutron flux and
- register fission fragments with detectors with the same (or well known) efficiencies.

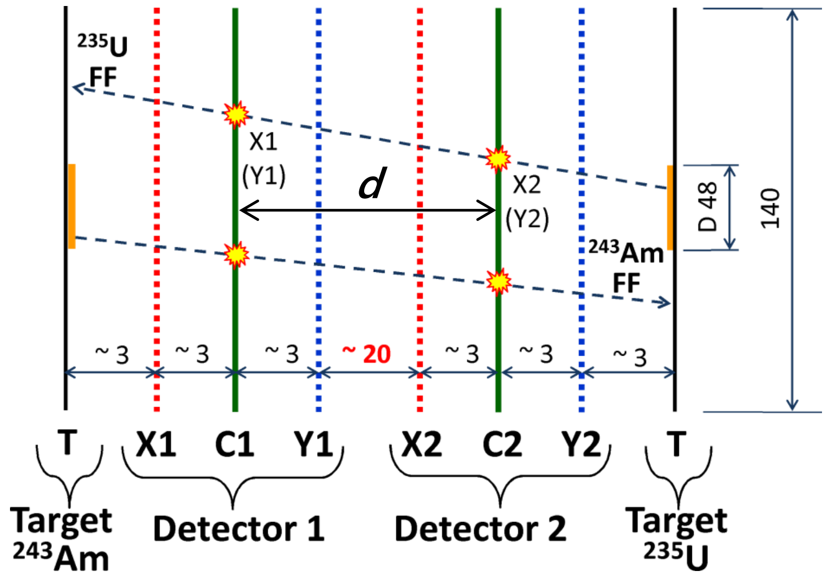

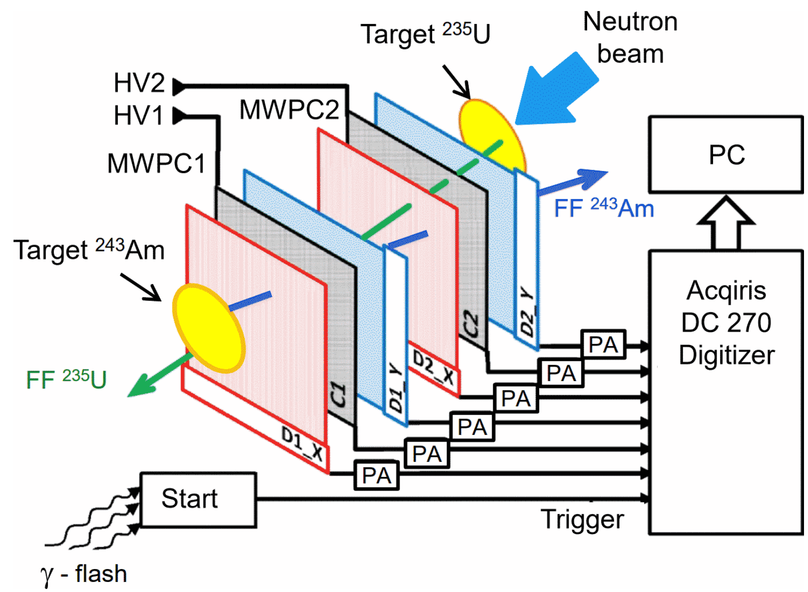

The setup consists of two position-sensitive low pressure multi-wire proportional counters. Targets are located on opposite sides of them.

Waveforms from 6 electrodes and from "Start" PM are recorded with 500 MHz 8 bit digitizer. →
7 timestamps and pulse heights → $x1, x2, y1, y2, T_{cathode1}, T_{cathode2}, T_{start}$ →

$$\cos(\theta) = \frac{d}{\sqrt{(x1-x2)^2+(y1-y2)^2+d^2}}$$

$$L/(T_{cathode} - T_{start}) \rightarrow E_n$$

Targets

Targets from ^{243}Am and ^{235}U were fabricat
by the "painting" method on aluminum su
sizes of the active layer were different (see

To ensure identical conditions for measure
equal shape samples in wide homogeneou
were placed on the active layers of the bot
a diameter of (48.0 ± 0.1) mm on the activ

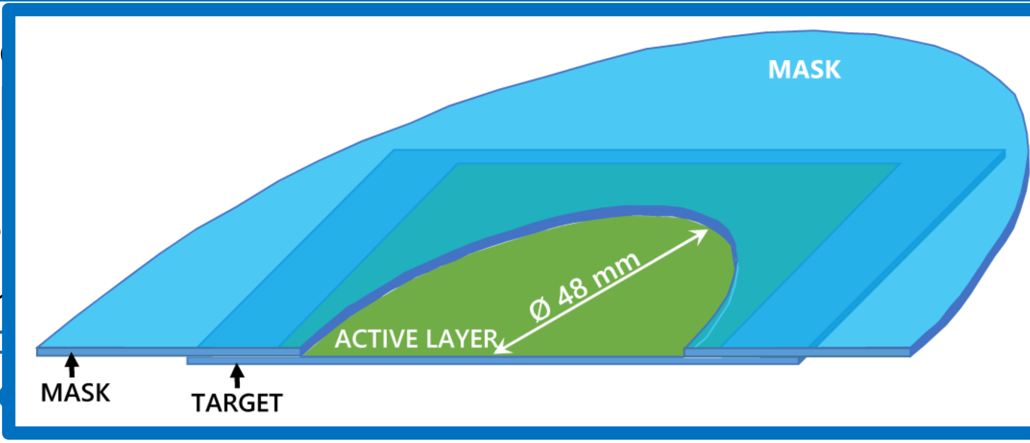

For to determine the scaling factor (N_{Am3}/N_{U5}), we have measured the isotope masses in these masked windows using α-spectroscopy.

Main isotope	^{235}U	^{243}Am
Thickness of active layer (μg/cm2)	203(11)	142(7)
Homogeneity of active layer	10%	10%
Sizes of active layer (mm)	50×100	Ø 82
Total target mass (mg)	10.15(51)	7.5(4)
Main isotope mass inside mask Ø 48 mm (mg)	3.480(48)	2.484(25)
Target activity inside the mask Ø 48 mm (Bq)	2.92×10^7	295
Scaling factor (N_{Am3}/N_{U5})	0.690(12)	

	^{235}U	^{243}Am
Isotope	Mass percentage (%)	
^{235}U	99.9920(10)	
^{234}U	0.0020(5)	
^{236}U	0.0040(5)	
^{238}U	0.0020(5)	
^{243}Am		99.13(10)
^{241}Am		0.75(1)
^{244}Cm		0.11(1)

Black- parameters given in manufacturer's certificates
Blue- more accurate parameters obtained by us using α-spectrometry

Method for selection of “true” fission events

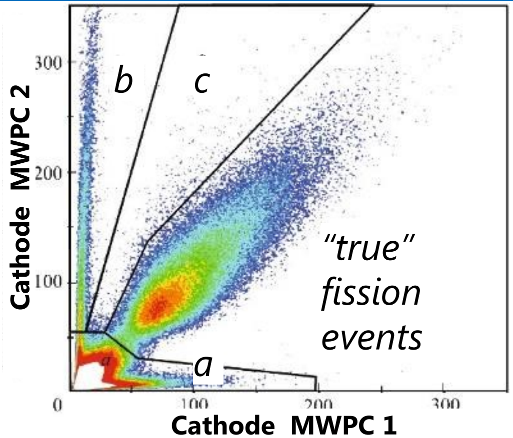

a. non-fission reactions in backing and α-partricles and noises
b. FFs “died” in MWPC 2 (first from the target)
c. FFs “died” on the cathode of MWPC 1 (second from the target)

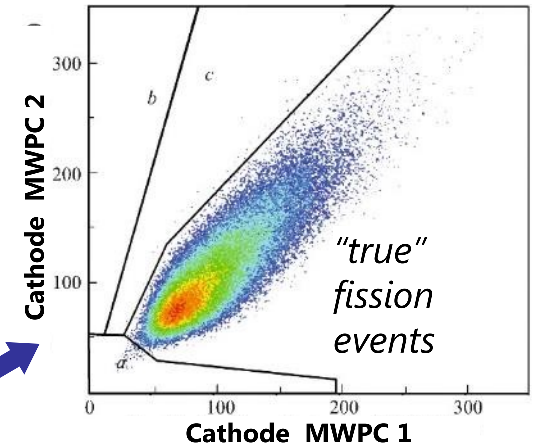

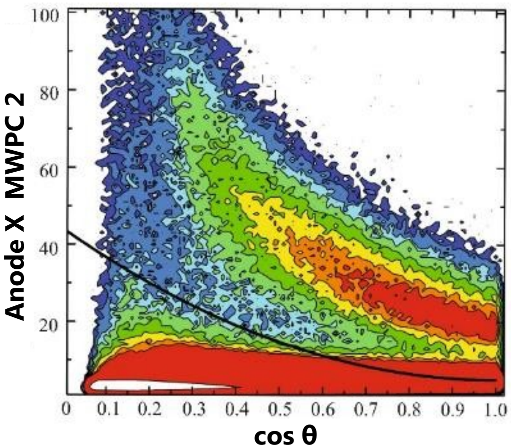

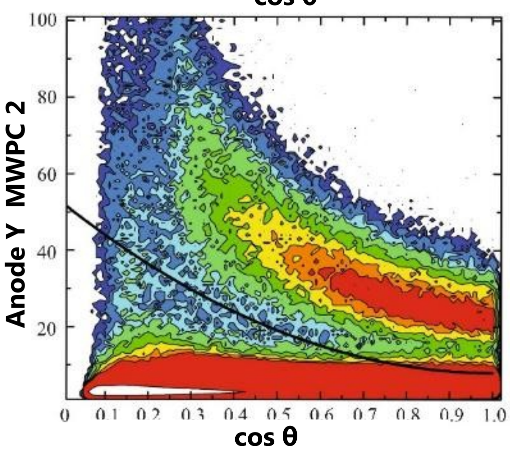

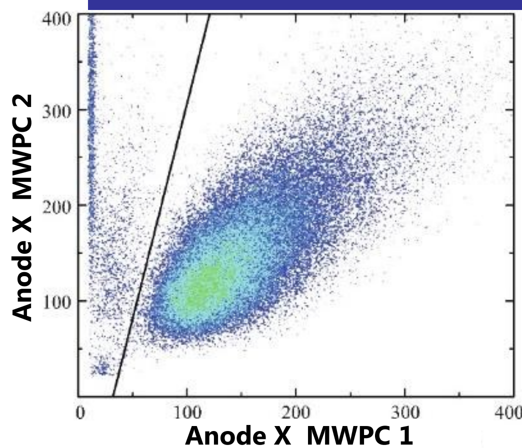

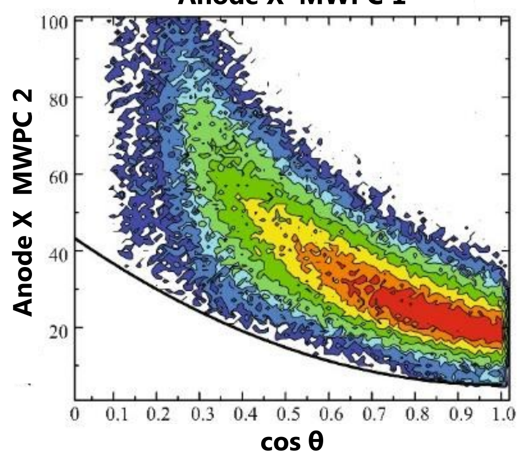

By applying a “proper” set of selection “cuts” to the 2-dimentional datasets –

(AnodeX_MWPC2 × cos(θ),
AnodeY_MWPC2 × cos(θ),
AnodeX_MWPC1 × AnodeX_MWPC1)

we are able to achieve complete rejection of non-fission events.

Amplitude spectra of signals from the MWPCs cathodes before the selection of "true" fission events (black) and after (red)

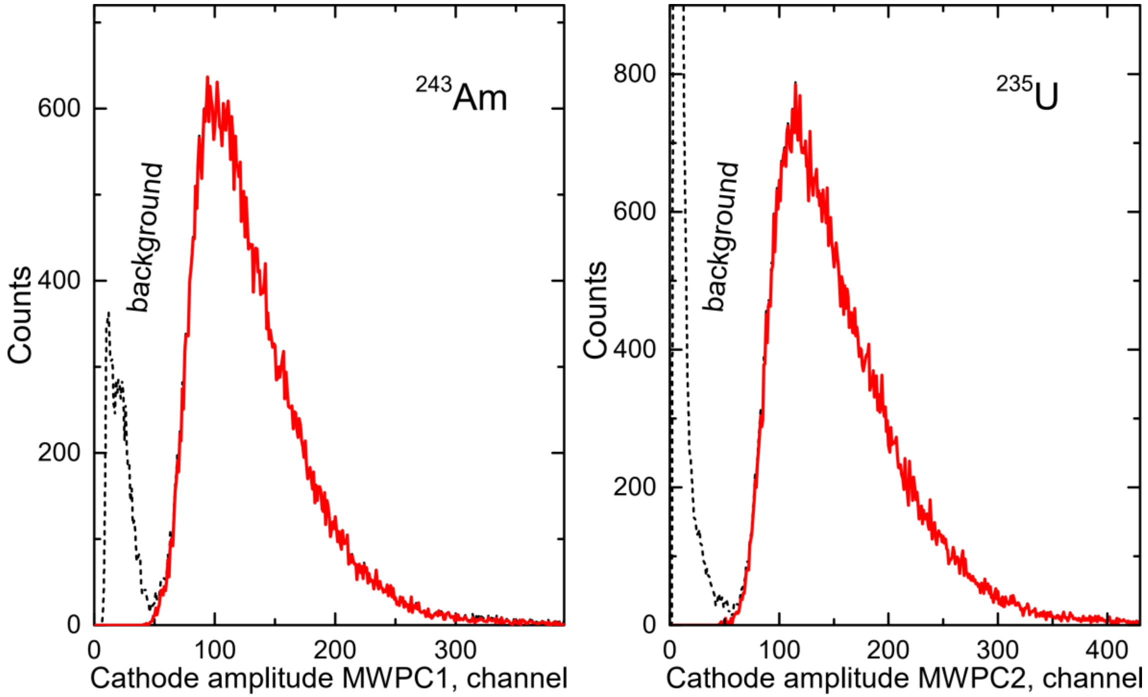

- It is remarkable that "true" fission events are completely separated from neutron-induced background reactions in the substrate of the target and in other materials of the detector, from α-particles and noise signals.
- Fission fragments are registered without any threshold cutoff

Admixture of spontaneous fission of ^{244}Cm in ^{243}Am target with isotropic angular distribution.

A small admixture of ^{244}Cm in the ^{243}Am target (0.11%) creates a background of spontaneous fission fragments. The background from spontaneous fissions of ^{244}Cm was 305±9 1/minute.

It was calculated based on the efficiency of detection of fission fragments, the spontaneous fission half-life for ^{244}Cm, and the mass of ^{244}Cm in “masked” target part, which was precisely determined in this work.

Thus, at neutron energy ~200 keV the share of spontaneous fission in the total fission fragments counts rate was about 70%, and at energies above 1 MeV, it does not exceed 0.2%.

The spontaneous fission background was subtracted from the time-of-flight spectra and from the measured angular distributions.

Separation of events from ^{235}U and ^{243}Am

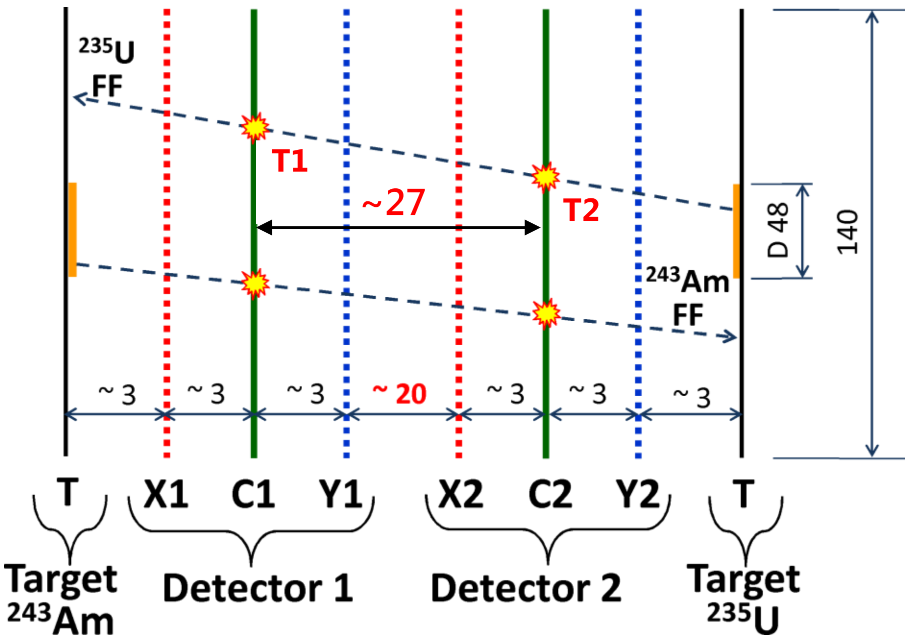

Time stamps T1 and T2 are derived from the waveforms of the signals from the two cathodes.

If the time mark T1 comes earlier than T2, then fragment from ^{243}Am passed the MWPCs from left to right.

If the time mark T1 arrives later than T2, then then fragment from ^{235}U passed the MWPCs from right to left.

In Time-of-flight spectrum (T1-T2) events from ^{243}Am and ^{235}U can be separated.

Time-of-flight spectrum of fission fragments of (left part) ^{243}Am and (right part) ^{235}U from the 500th channel at various angles θ

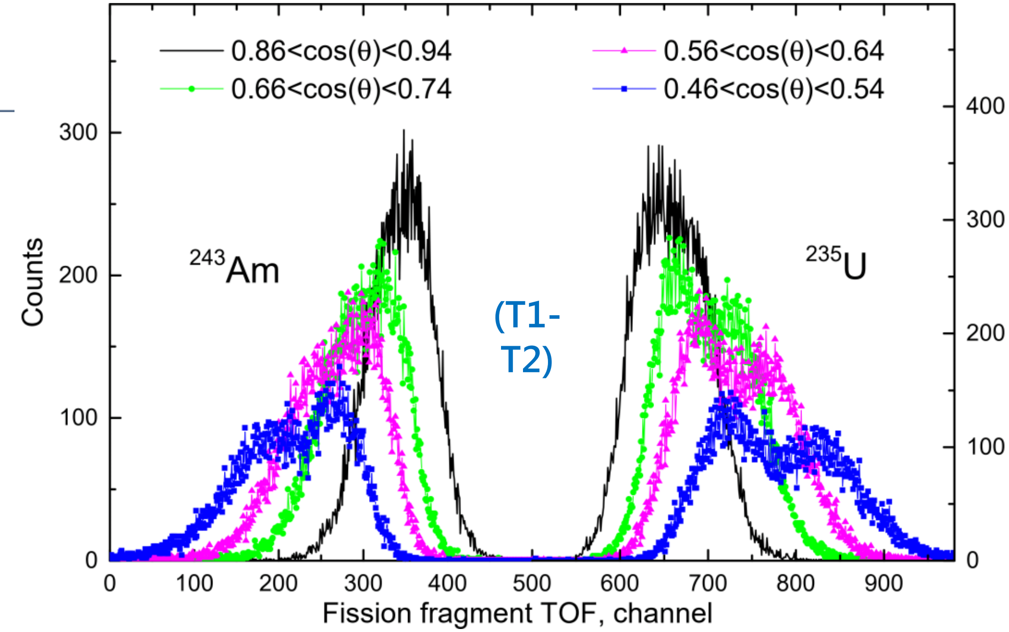

Monte-Carlo efficiency simulation in real setup geometry

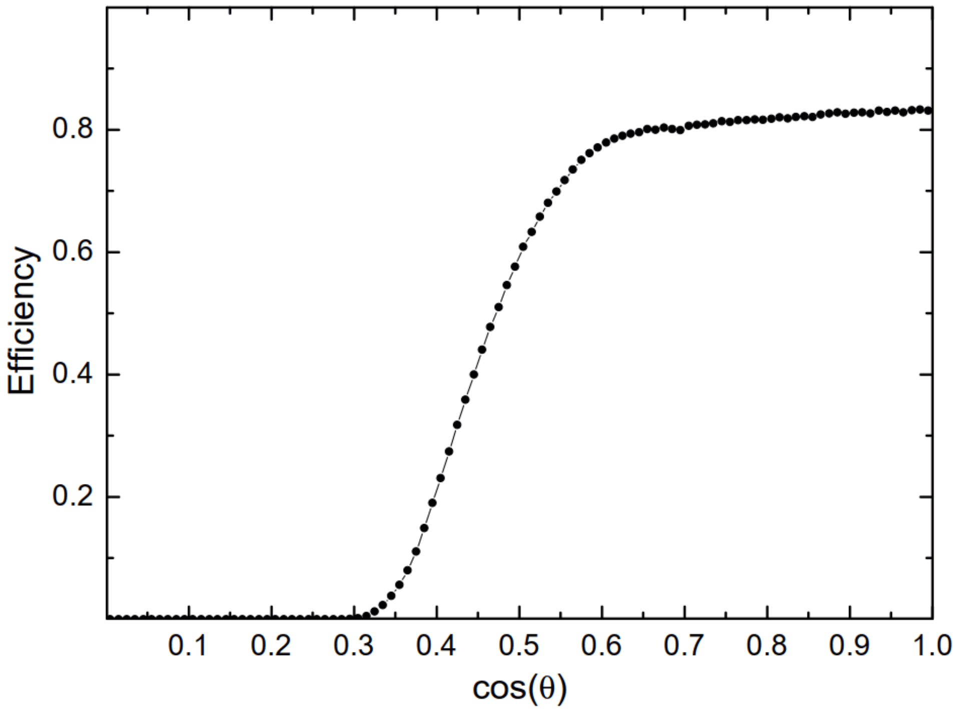

$$W_{correct}(\theta) = \frac{W_{exp}(\theta}{\text{Efficiency}}$$

The geometrical efficiency of detection of fission fragments by the array of two MWPCs was calculated using the Monte-Carlo method taking into account

- the actual geometry of the MWPCs,
- the size of the active spot on the target separated by the "mask",
- the spatial resolution of the MWPCs.

The fission fragment detection geometrical efficiency was ~43%, and the maximum fragment detection angle relative to the normal to the MWPC electrode plane was ~72^{o}.

Results: angular distributions of FF from $^{243}Am(n,f)$

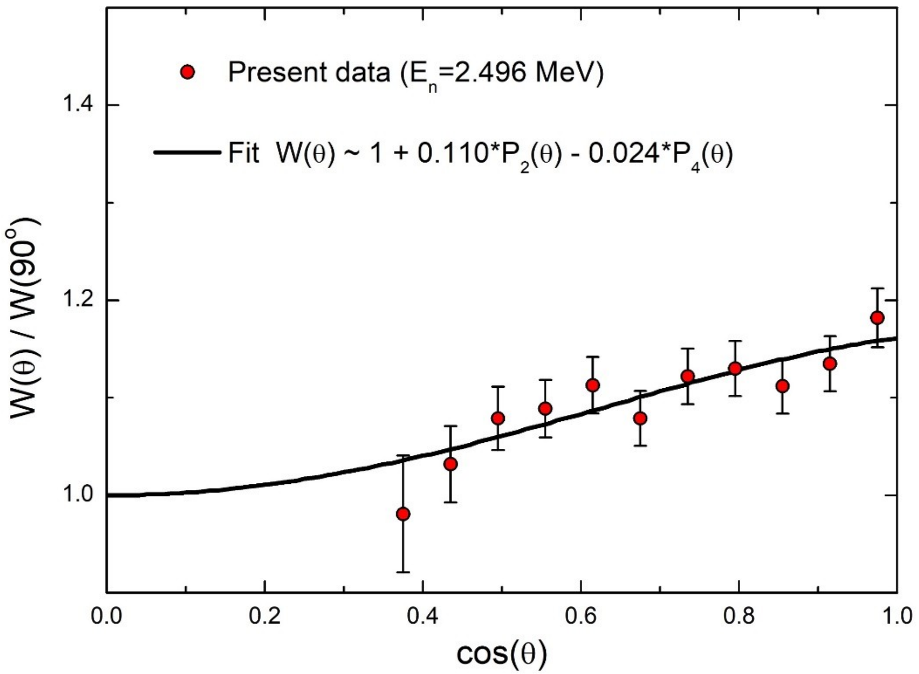

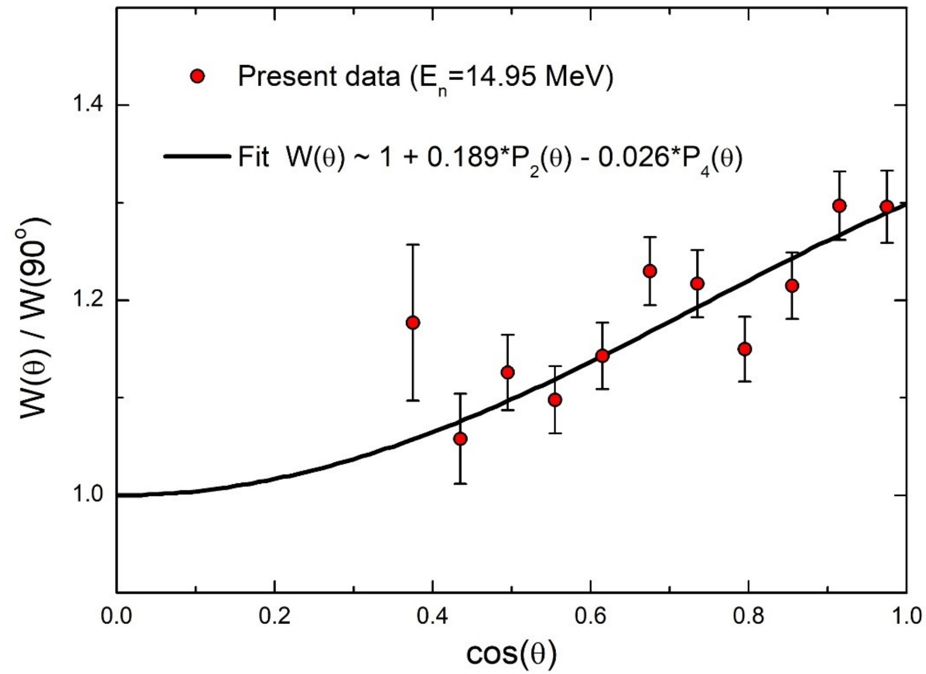

For each neutron energy point E_n, the angular distributions $W(\theta)$ measured at cos(θ) > 0.35 were approximated by the function of the sum of even Legendre polynomials up to the 4th degree :

$$W(\theta) = A_0\left[1 + \sum_{n=1}^{2} A_{2n}P_{2n}(\cos(\theta))\right]$$

The anisotropy of the angular distribution of fission fragments is determined using the coefficients A_2 and A_4 for the corresponding Legendre polynomials :

$$W(0°)/W(90°) = \frac{1 + A_2 + A_4}{1 - \frac{1}{2}A_2 + \frac{3}{8}A_4}$$

Results: anisotropy of FFs emission in ^{243}Am

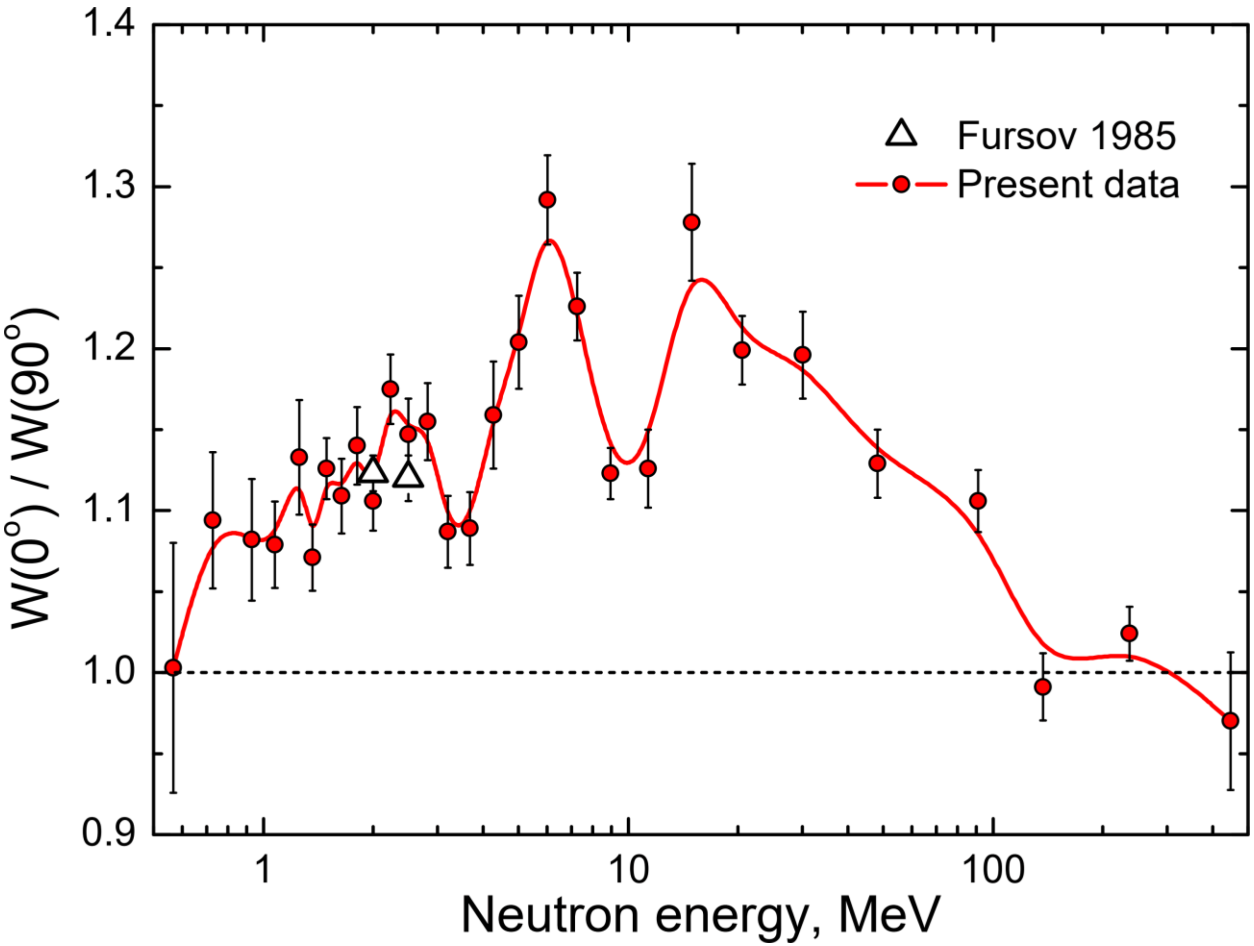

$$W(\theta) = A_0\left[1 + \sum_{n=1}^{2} A_{2n}P_{2n}(\cos(\theta))\right]$$

$$W(0^\circ)/W(90^\circ) = \frac{1 + A_2 + A_4}{1 - \frac{1}{2}A_2 + \frac{3}{8}A_4}$$

The indicated errors are statistical.

The systematic error in determining the anisotropy in this experiment, which is related to the finite angular resolution of the arrays with MWPC and the uncertainty in the geometry of the experiment, is ~0.5%.

The systematic error associated with the approximation used for fitting is 1-1.5%

- ✓ There is the only one paper by Fursov_1985 et al. (Van der Graaff, IPPE, Russia), where the anisotropy in the fission of ^{243}Am was measured in two points for neutrons with energies 2 and 2.5 MeV.
  The results of this work agree with our data within the error limits.

Status of the anisotropy of FFs emission measurements for 2023

	GNEIS, PNPI	n-TOF, CERN	NIFFTE, WNR, LANSCE
^{232}Th	JETP Letters, 102, 203 (2015) EXFOR #41608002	Nucl. Data Sheets, 119, 35 (2014) EXFOR #23209	
^{233}U	JETP Letters, 104, 365 (2016) EXFOR #41616006		
^{235}U	JETP Letters, 102, 203 (2015) EXFOR #41608003	EPJ Web of Conf. 111, 10002 (2016)	D. Hensle et al., Phys. Rev. C 102, 014605 (2020) EXFOR #14660002
^{236}U	Measurements completed		
^{238}U	JETP Letters, 102, 203 (2015) EXFOR #41608004	EPJ Web of Conf. 111, 10002 (2016)	D. Hensle et al., Phys. Rev. C 102, 014605 (2020) EXFOR #14660003
^{237}Np	JETP Letters 110, 242 (2019) EXFOR #41686002		
^{239}Pu	JETP Letters, 107, 521 (2018) EXFOR #41658003		
^{240}Pu	JETP Letters, 112, 323 (2020) EXFOR #41737002		
^{242}Pu	Measurements completed		
^{243}Am	Measurements completed		
^{nat}Pb	JETP Letters, 107, 521 (2018) EXFOR #41658004		
^{209}Bi	JETP Letters, 104, 365 (2016) EXFOR #41616007		

12 nuclei are measured
9 are published and
presented in EXFOR

Ratio of the fission cross sections of ^{243}Am and ^{235}U according to our measurements and other experimental data taken from the EXFOR database

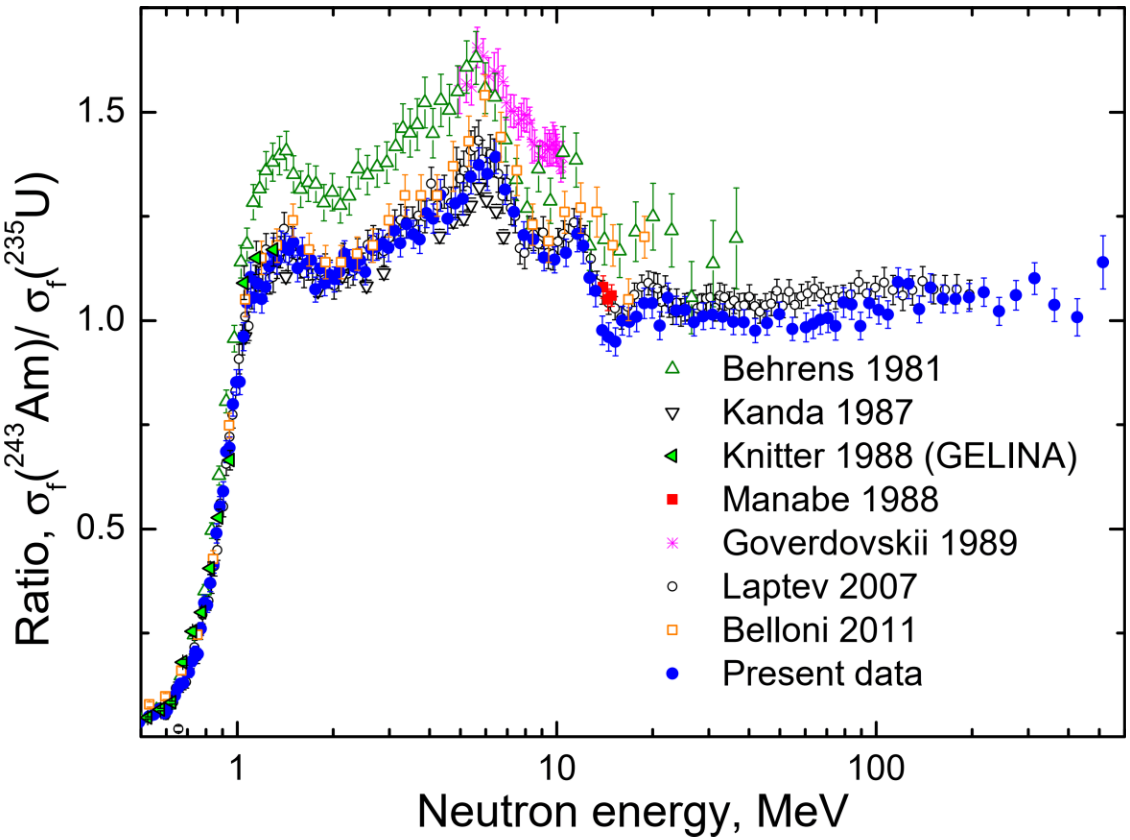

We have determined the scaling factor N_{Am3}/N_{U5} - the ratio of the number of ^{243}Am and ^{235}U nuclei in the targets.

Both of these targets were placed in a wide and uniform neutron flux, and fission fragments were registered by the same pair of the detectors with the equal efficiency.

Necessary corrections were applied:

- for the geometrical efficiency dependence on angular anisotropy of fragment emission,
- for the isotopic composition of the targets,
- and for the background from spontaneous fission events.

We get the ratio of the fission cross sections of ^{243}Am and ^{235}U.

Ratio of the fission cross sections of ^{243}Am and ^{235}U according to our measurements and other experimental data taken from the EXFOR database

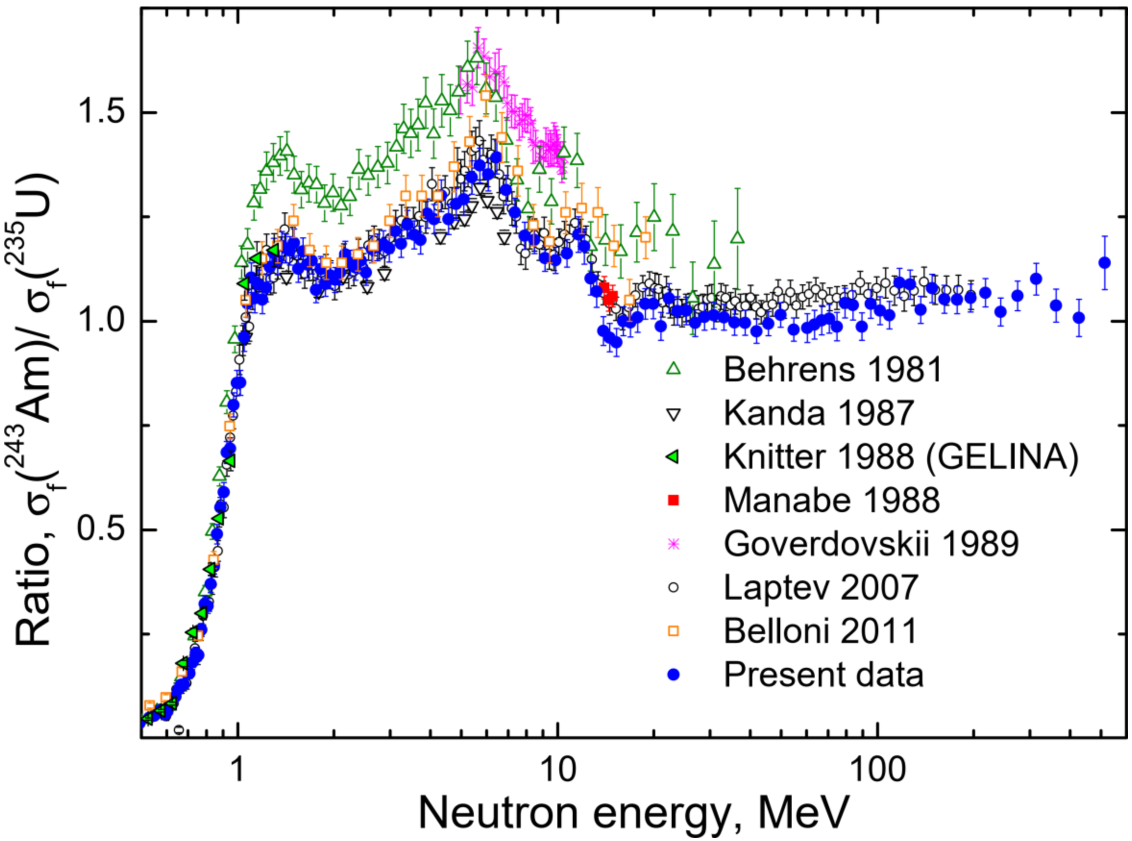

The shape of the energy dependence of the ratio obtained in this work coincide with the other data for E_n < 30 MeV, but the Behrens_1981 and Goverdovskii_1989 data are ~15% higher.

For E_n > 30 MeV the ratio obtained in this work can be compared only with the results of Laptev_2007.

The work Laptev_2007 was also performed on the GNEIS spectrometer using a fission ionization chamber as a detector.

The results coincide reasonably well in the entire range of neutron energies.

Unfortunately, in the work Laptev_2007 the ratio was not normalized to the number of nuclei in the targets; instead, the authors normalized the ratio they obtained to the ratio of the fission cross sections of ^{243}Am and ^{235}U taken from the ENDF/B-VII files for some neutron energy ranges.

List of uncertainties

Statistical uncertainties	60–3 % (0.2-0.9 MeV) 2–3 % (above 0.9 MeV)
Attenuation of the neutron flux	<0.3 %
Anisotropy	~1 %
Purity of targets (isotope composition)	1 % (below 0.8 MeV) 0.4 % (0.8–1.5 MeV 0.1 % (above 1.5 MeV)
Efficiency of multiwire proportional counters (geometrical uncertainty)	0.3 %
Scaling factor (N_{Am3}/N_{U5})	1.7 %
Total error	~3.2 %
Uncertainty of the ^{235}U "standard" cross section (A.D. Carlson et al., Nuclear Data Sheets 148, 143, 2018)	
$\sigma_f(^{235}U)$	1.3–1.5 % (below 20 MeV) 1.5–4.8 % 20–200 MeV 5–7 % (above 200 MeV)

The total average systematic error is ~2%
and it is mainly determined by
the uncertainty of the correction for the anisotropy of fragment emission ~1.0%
and the uncertainty of the scaling factor ~1.7%.

Fission cross sections of ^{243}Am obtained in this work and from other experiments. The solid and dashed line consist of the estimates from the ENDF/B-VIII.0 and JEFF-3.3 library

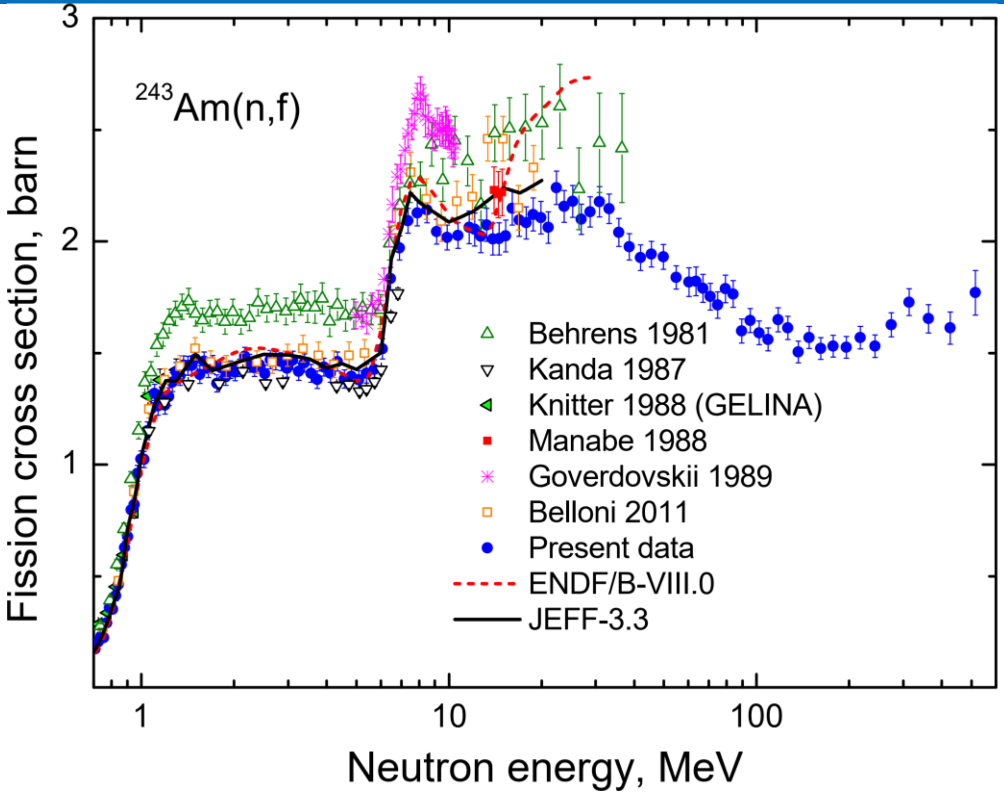

For all experimental data shown in the figure, the ^{243}Am cross section was determined as the product of the measured ratio R and the $\sigma_f(^{235}U)$– existing standard of the $^{235}U(n,f)$ fission cross section.

It can be seen that the ^{243}Am fission cross section obtained in this work mostly agrees with the results of Kanda_1987, Manabe_1988, Belloni_2011, and Knitter_1988 (obtained at GELINA using TOF method),

while the data from Behrens_1981 and Goverdovskii_1989 are ~15% higher.

Taking into account that the uncertainty of the scaling of the ratio R, stated in these works, is only 2-3%, one can talk about the presence of unknown systematic errors.

Fission cross sections of ^{243}Am obtained in this work and from other experiments. The solid and dashed line consist of the estimates from the ENDF/B-VIII.0 and JEFF-3.3 library – low neutron energies

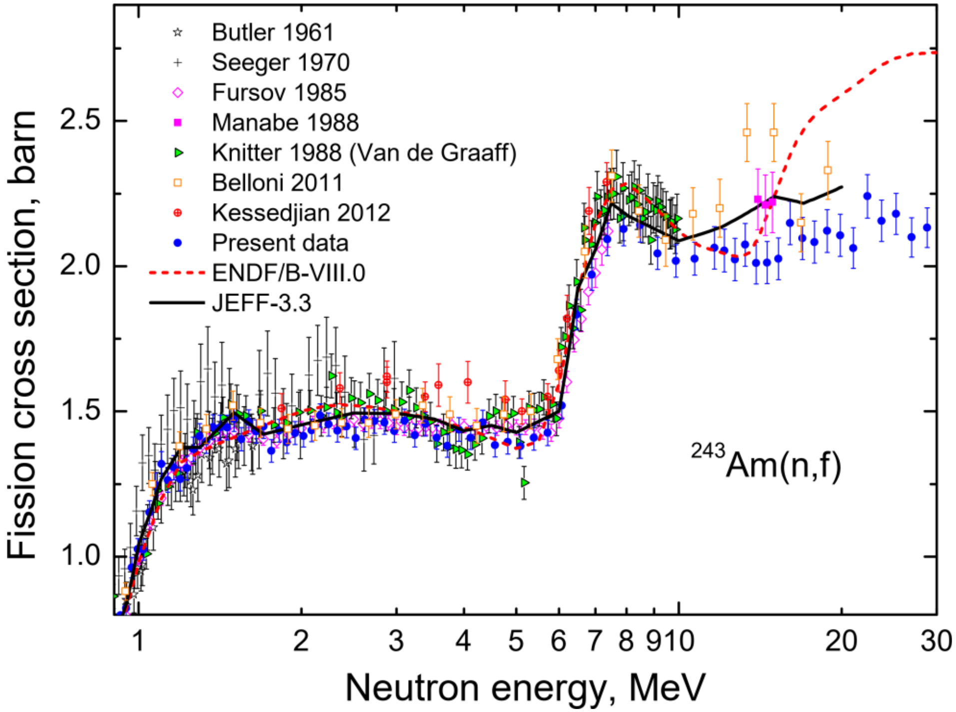

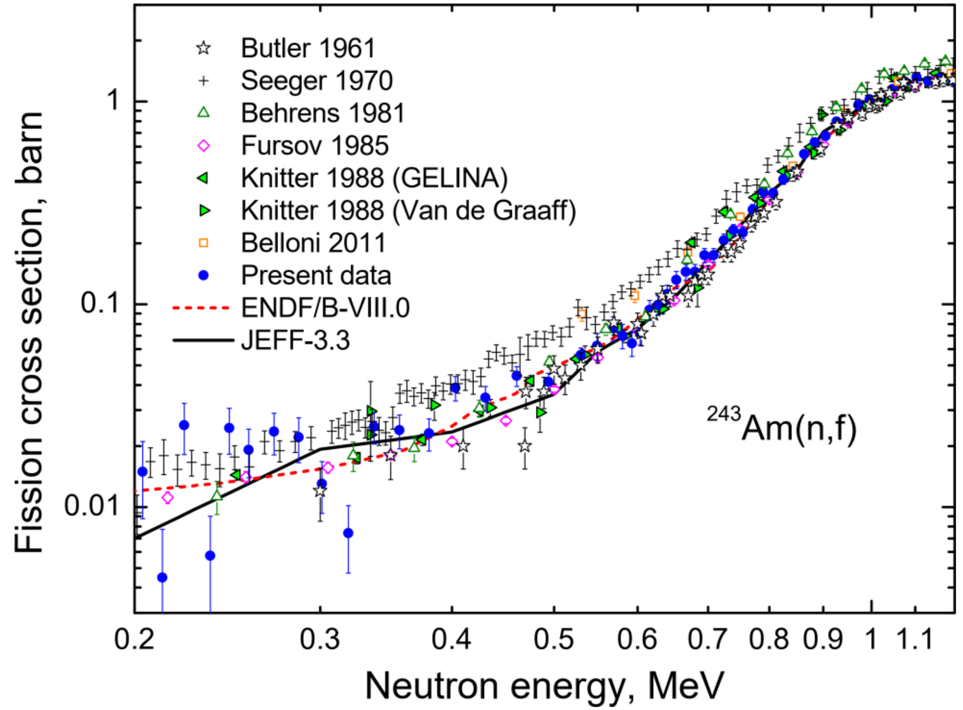

Some of the datasets for representation on the Figure were obtained from the data given in the corresponded papers after some necessary renormalization (Knitter_1988-VdG, Fursov_1985).

As can be seen from the comparison of the presented results, in general, within the total error bars, there is agreement between the data of our work and the previous data, as well as the estimates from the ENDF/B-VIII.0 library and JEFF-3.3. The exception is Seeger_1970 data (nuclear explosion), whose data have a systematic shift in energy of about 50 keV compared to others.

Ratio of the fission cross sections of ^{243}Am obtained in this work and in other measurements to the estimate for this cross section from the JEFF-3.3 library

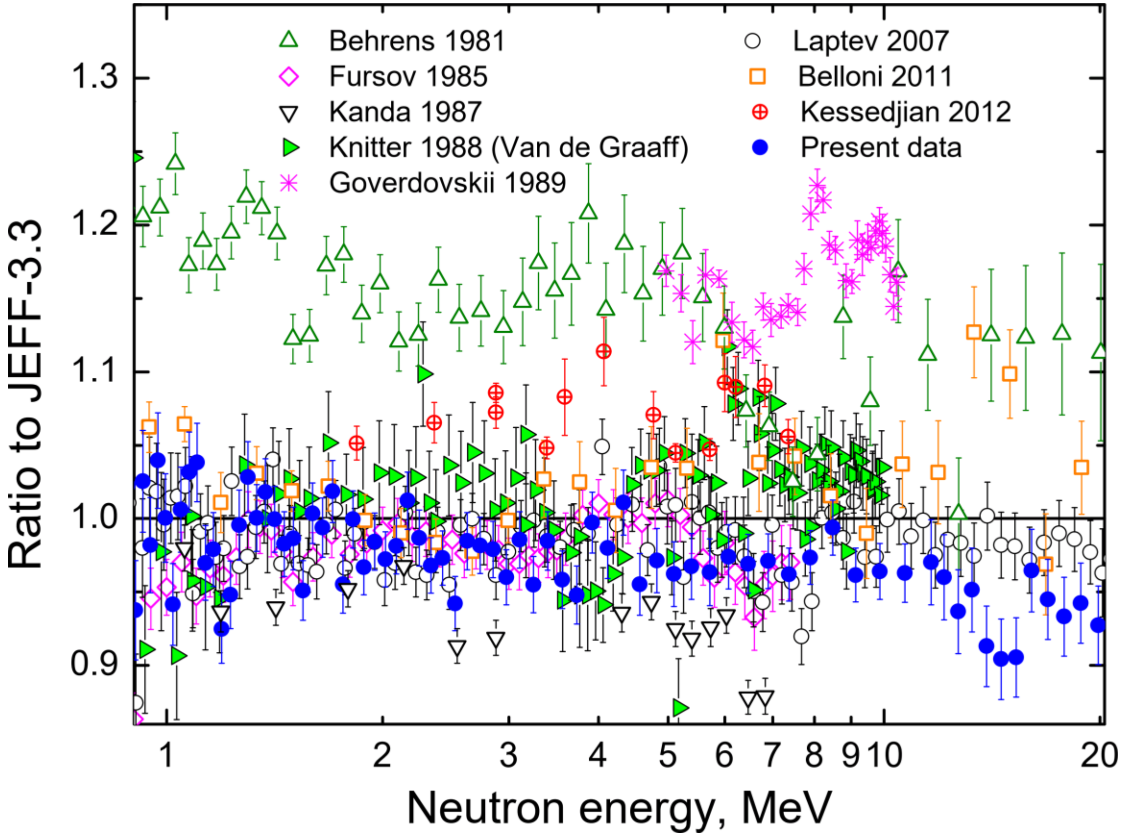

In the neutron energy range 1–20 MeV, the ratio between the experimental data and the estimate from JEFF-3.3 is approximately constant within the error bars. The average deviation for all data except Behrens_1981, Kanda_1987 and Goverdovskii_1989 doesn't exceed the experimental accuracy of determining the scaling factor associated with the target masses, the detection efficiency and the neutron flux. This behavior indicates that the shape of the ^{243}Am fission cross section from the JEFF-3.3 library quite correctly describes the available experimental data, and the observed difference in some data is apparently due to the inaccuracy of the absolute normalization of the measured ratios of the fission cross sections of ^{243}Am and ^{235}U in these works.

Ratio of the fission cross sections of ^{243}Am obtained in this work and in estimates from 4 national data libraries to the estimate for this cross section from the JEFF-3.3 library

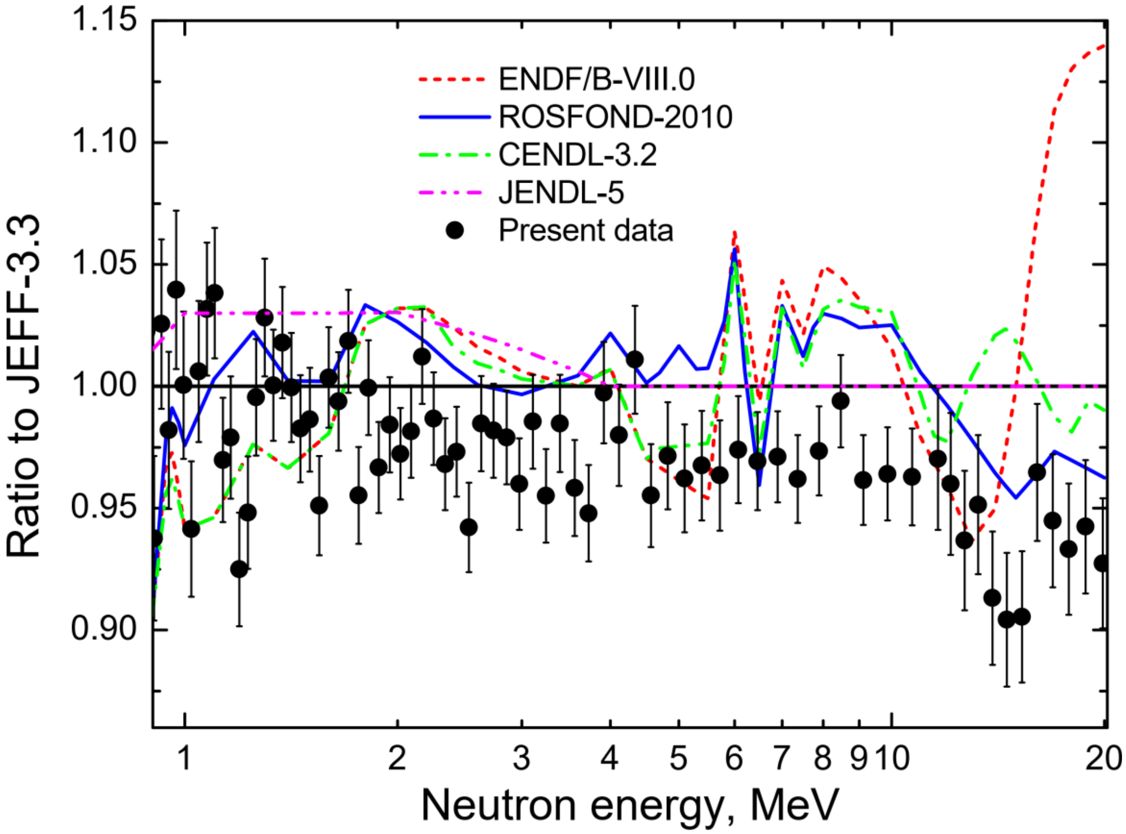

In the specified energy interval, all estimates agree within ~5% with the estimate from the JEFF-3.3 library, with the exception of the ENDF/B-VIII.0 estimate, the deviation of which at neutron energies above 14 MeV begins to grow and reaches 15% for neutron energies of about 20 MeV.

Summary

- In this work, new measurements of the ^{243}Am fission cross section are carried out on the neutron TOF-spectrometer GNEIS at Petersburg Nuclear Physics Institute of National Research Centre «Kurchatov Institute» in the neutron energy range up to 500 MeV
- The neutron induced fission cross section of ^{243}Am was obtained in a wide energy range with the experimental uncertainty 3-4%.
- The obtained data on the fission cross section are mostly consistent with the results of earlier experimental works in the energy range up to 20 MeV, and above 20 MeV – the shape of the fission cross section agrees with the only existing old GNEIS data (Laptev_2003).
- The differences between the existing experimental data seem to be mostly related to uncertainties in the detection efficiency of the fission fragment detectors used, the neutron flux, and the target masses (number of nuclei).
- The anisotropy of the angular distributions of ^{243}Am fission fragments are measured for the first time in the energy range 0.7-400 MэВ.

Thank you for attention

Angular distributions of fission fragments

Transition states at the saddle point of highly deformed fissioning nuclei:

$$W^J_{M,K}(\theta) = \frac{2J+1}{2}\left|d^J_{M,K}\right|^2$$ (wave function of axial top)

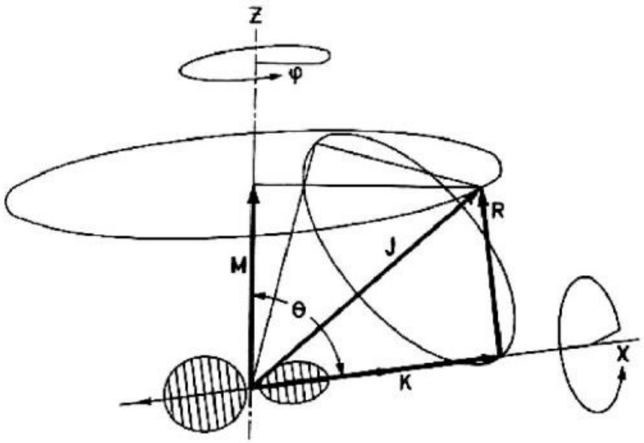

For low excitation energies we need a proper sum over non-uniform *M* distribution, and few available *J*, *K* (fission channels) and finally:

$$W(\theta) \sim \sum_{n_{even}} A_n P_n(\cos\theta)$$

At high excitations with many opened fission channels one can use statistical model for the *K* projection distribution – $\rho(K)$:

$$\rho(K) \sim \exp\left(-\frac{E_{rot}}{T}\right); \quad E_{rot} = \frac{\hbar^2[J(J+1)-K^2]}{2J_\perp} + \frac{\hbar^2 K^2}{2J_\parallel}; \quad T = \sqrt{E^*/a_f}$$

$$\rho(K) \sim \exp\left(-\frac{K^2}{2K_0^2}\right)$$, where $K_0^2 = \frac{J_{eff}T}{\hbar^2}$, and $J_{eff} = \frac{J_\perp J_\parallel}{J_\perp - J_\parallel}$

In statistical model:

$$W(\theta) \sim 1 + A\cos^2\theta \qquad \frac{W(0^o)}{W(90^o)} = A + 1 \approx \frac{\langle J^2 \rangle}{4K_0^2} + 1$$

Experimental setup

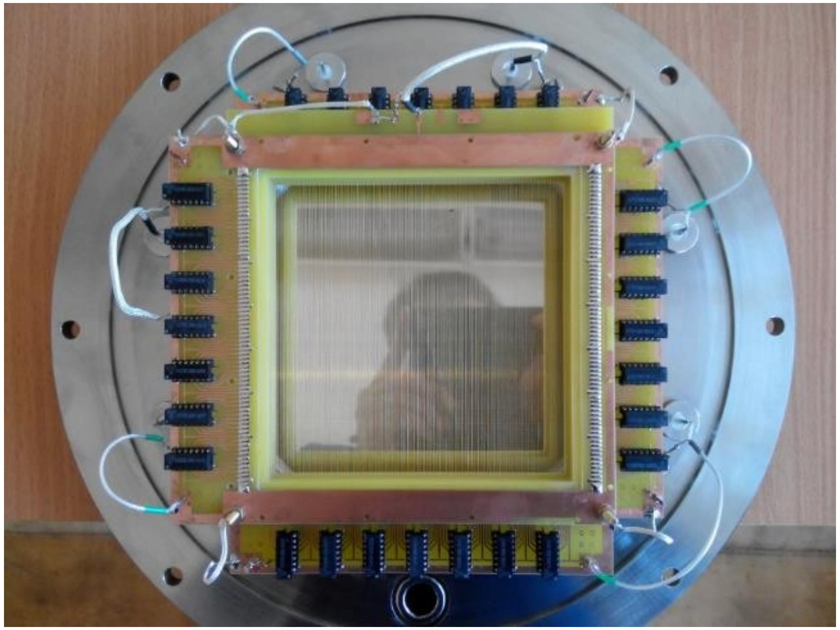

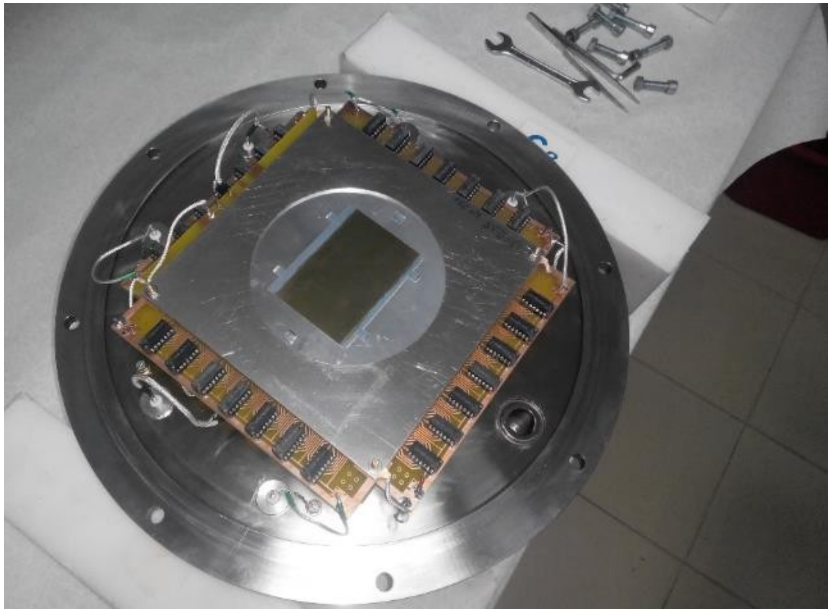

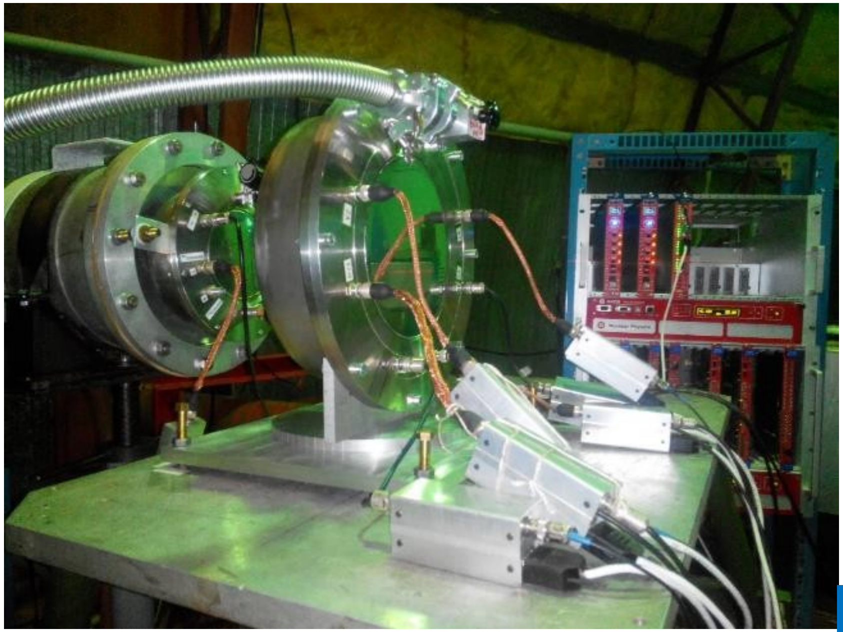

References

[1]{Gen4_2014}
The Generation IV International Forum (GIF), Technology Roadmap Update for Generation IV Nuclear Energy Systems (OECD-NEA, Paris, 2014).
[2]{Glebov_2020}
А.П. Глебов, ВАНТ, Серия: Ядерно-реакторные константы, Вып. 1, 77 (2020).
[3]{ADS_2015}
Report IAEA-TECDOC series, no. 1766. Vienna, IAEA, 2015.
[4]{Gulevich_2020}
A.V. Gulevich, V.A. Eliseev, D.A. Klinov, L.V. Korobeinikova, M.V. Kryachko, V.A. Pershukov, V.M. Troyanov, At. Energy {\bf 128}, 88 (2020).
[5]{WPEC26_2008}
Uncertainty and target accuracy assessment for innovative system using recent covariance data evaluations, Nuclear Science/WPEC-26, NEA No. 6410. OECD-NEA, 2008 (ISBN 978-92-64-99053-1).
[6]{SPAR-IV_2021}
Report IAEA-TECDOC series, no. 1975. Vienna, IAEA, 2021.
[7]{Carlson_2018}
A.D. Carlson, V.G. Pronyaev, R. Capote {\it et al.}, Nuclear Data Sheets {\bf 148}, 143 (2018).
[8]{Marcinkevicius_2015}
B. Marcinkevicius, S. Simakov, V. Pronyaev, IAEA Report No. INDC(NDS)-0681 (2015).
https://nds.iaea.org/standards/
[9]{Butler_1961}
D.K. Butler, R.K. Sjoblom, Phys. Rev. {\bf 124}, 1129 (1961). EXFOR 12543003.
[10]{Seeger_1970}
P.A. Seeger, Los Alamos Sci. Lab. Rep. LA-4420, p.138 (1970). EXFOR 10063004.
[11]{Behrens_1981}
J.W. Behrens, J.C. Browne, Nucl. Sci. Eng. {\bf 77}, 444 (1981). EXFOR 10652003.

References

[12]{Fursov_1985}
B.I. Fursov, E.Yu. Baranov, M.P. Klemyshev, B.F. Samylin, G.N. Smirenkin, Yu.M. Turchin, Soviet Atomic Energy {\bf 59}, 899 (1985). EXFOR 40837003. EXFOR 40837006.
https://doi.org/10.1007/BF01133085
[13]{Kanda_1987}
K. Kanda, H. Imaruoka, H. Terayama, Y. Karino, N. Hirakawa, Jour. of Nuclear Science and Technology {\bf 24}, 423 (1987). EXFOR 22044002.
http://dx.doi.org/10.3327/jnst.24.423
[14]{Knitter_1988}
H. Knitter, C. Budtz-Jorgensen, Nucl. Sci. Eng. 99, 1 (1988). EXFOR 22032002 (Van de Graaff).
[15]{Manabe_1988}
F. Manabe, K. Kanda, T. Iwasaki, H. Terayama, Y. Karino, M. Baba, N. Hirakawa, Fac. of Engineering, Tohoku Univ. Tech. Report, Vol.52, Issue.2, p.97 (1988). EXFOR 22282009.
[16]{Goverdovskii_1989}
A.A. Goverdovskii, A.K. Gordyushin, B.D. Kuz'minov, V.F. Mitrofanov, A.I. Sergachev, S.M. Solov'ev, T.E. Kuz'mina, Soviet Atomic Energy {\bf 67}, 524 (1989). EXFOR 41058002.
[17]{Kessenjian_2012}
G. Kessedjian, G. Barreau, M. Aïche, B. Jurado, A. Bidaud, S. Czajkowski, D. Dassié, B. Haas, L. Mathieu, L. Tassan-Got, J.N. Wilson, F.-J. Hambsch, S. Oberstedt, I. AlMahamid, J. Floyd, W. Lukens, D. Shuh, Phys. Rev. C {\bf 85}, 044613 (2012). EXFOR 22993003, 22993004, 22993005.
[18]{Belloni_2011}
F. Belloni, M. Calviani, N. Colonna, P. Mastinu, P.M. Milazzo, U. Abbondanno, G. Aerts, H. Álvarez, F. Alvarez-Velarde, S. Andriamonje, (n$\underline{}$TOF collaboration), Eur. Phys. J. A {\bf 47}, 160 (2011). EXFOR 23148002.
[19]{Laptev_2003}
A.B. Laptev, A.Yu. Donets, A.V. Fomichev, A.A. Fomichev, R.C. Haight, O.A. Shcherbakov, S.M. Soloviev, Yu.V. Tuboltsev, A.S. Vorobyev, Nuclear Physics A {\bf 734}, Issue.1, p.E45 (2004).

References

[20]{Abrosimov_1985}
N.K. Abrosimov, G.Z. Borukhovich, A.B. Laptev {\it et al.}, Nucl. Instrum. Methods Phys. Res. A {\bf 242}, 121 (1985).
[21]{Shcherbakov_2018}
O.A. Shcherbakov, A.S. Vorobyev, and E.M. Ivanov, Phys. Part. Nuclei {\bf 49}, 81 (2018).
[22]{{Fomichev_2005}
A.V. Fomichev, V.N. Dushin, S.M. Soloviev, A.A. Fomichev, S. Mashnik, Los Alamos National Laboratory Reports, No. LA-UR-05-1533 (2005).
[23]{{Laptev_2007}
A.B. Laptev, O.A. Shcherbakov, A.S. Vorobyev, R.C. Haight, A.D. Carlson, in: {\sl Proceedings of the Conference on Fission and Properties of Neutron-Rich Nuclei}, Sanibel Island (2007), edited by J.H. Hamilton, A.V. Ramayya, H.K. Carter (World Scientific, 2008) p. 462. EXFOR 41487015.
[24]{{Vorobyev_2023}
A.S. Vorobyev, A.M. Gagarski, O.A. Shcherbakov, L.A. Vaishnene, and A.L. Barabanov, JETP Letters {\bf 117(8)}, 526 (2023).
[25]{{Gagarski_2017}
A.M. Gagarski, A.S. Vorobyev, O.A. Shcherbakov, L.A. Vaishnene, in: {\sl Proc. of XXIV International Seminar on Interaction of Neutrons with Nuclei ``Fundamental Interactions and Neutrons, Nuclear Structure, Ultracold Neutrons, Related Topics''} (ISINN-24, Dubna, May 24 -27, 2016), Dubna, JINR, E3-2017-8, 2017, p. 343-350.
[26]{{Vorobyev_2015}
A.S. Vorobyev, A.M. Gagarski, O.A. Shcherbakov, L.A. Vaishnene, and A.L. Barabanov, JETP Letters {\bf 102(4)}, 203 (2015). EXFOR 41608004.
[27]{{Vorobyev_2016}
A.S. Vorobyev, A.M. Gagarski, O.A. Shcherbakov, L.A. Vaishnene, and A.L. Barabanov, JETP Letters {\bf 104(6)}, 365 (2016).
[28]{{Vorobyev_2018}
A.S. Vorobyev, A.M. Gagarski, O.A. Shcherbakov, L.A. Vaishnene, and A.L. Barabanov, JETP Letters {\bf 107(9)}, 521 (2018).

References

[29]{{Vorobyev_2019}
A.S. Vorobyev, A.M. Gagarski, O.A. Shcherbakov, L.A. Vaishnene, and A.L. Barabanov, JETP Letters {\bf 110(4)}, 242 (2019).
[30]{{Vorobyev_2020}
A.S. Vorobyev, A.M. Gagarski, O.A. Shcherbakov, L.A. Vaishnene, and A.L. Barabanov, JETP Letters {\bf 112(6)}, 323 (2020).
[31]{LCN}
Evaluated Nuclear Structure Data File, https://www.nndc.bnl.gov/ensdf
[32]{Otuka_2014}
N. Otuka, E. Dupont, V. Semkova {\it et al.}, Nuclear Data Sheets {\bf 120}, 272 (2014). https://www-nds.iaea.org/exfor/
[33]{Brown_2018}
D.A. Brown, M.B. Chadwick, R. Capote {\it et al.}, Nuclear Data Sheets {\bf 148}, 1 (2018).
[34]{OECD_2018}
OECD and NEA, The Joint Evaluated Fission and Fusion File (JEFF) – Version 3.3 (OECD-NEA, Paris, 2018), https://www.oecd-nea.org/dbdata/jeff/jeff33/
[35]{Zabrodskaya_2007}
S.V. Zabrodskaya, A.V. Ignatyuk, V.N. Koscheev {\it et al.}, VANT. Ser.: Yadernye konstanty. iss. 1-2, 3 (2007) (in Russian). https://www-nds.iaea.org/exfor/endf.htm
[36]{Yankov_1983}
G.B. Yankov, Technical Reports Series No. 227, p. 39, IAEA, Vienna (1983).
[37]{Iwamoto_2020}
O. Iwamoto, N. Iwamoto, K. Shibata {\it et al.}, EPJ Web of Conferences {\bf 239}, 09002 (2020). https://www-nds.iaea.org/exfor/endf.htm
[38]{Ge_2020}
Zhigang Ge, Ruirui Xu, Haicheng Wu {\it et al.},EPJ Web of Conference {\bf 239}, 09001 (2020). https://www-nds.iaea.org/exfor/endf.htm